Biochemical and Biophysical Research Communications xxx (2017) 1–7

Contents lists available at ScienceDirect

Biochemical and Biophysical Research Communications

journal homepage: www.elsevier.com/locate/ybbrc

Identification and characterization of UDP-mannose in human cell lines and mouse organs: Differential distribution across brain regions and organs

Kazuki Nakajima [a, b], Yasuhiko Kizuka [b], Yoshiki Yamaguchi [c], Yoshio Hirabayashi [d], Kazuo Takahashi [e], Yukio Yuzawa [e], Naoyuki Taniguchi [b, *]

[a] Department of Academic Research Support Promotion Facility, Center for Research Promotion and Support, Fujita Health University, Toyoake, Aichi 470-1192, Japan
[b] Disease Glycomics Team, Systems Glycobiology Research Group, RIKEN-Max Planck Joint Research Center, RIKEN Global Research Cluster, 2-1 Hirosawa, Wako, Saitama 351-0198, Japan
[c] Structural Glycobiology Team, Systems Glycobiology Research Group, RIKEN-Max Planck Joint Research Center, RIKEN Global Research Cluster, 2-1 Hirosawa, Wako, Saitama 351-0198, Japan
[d] Molecular Membrane Neuroscience, RIKEN Brain Science Institute, 2-1 Hirosawa, Wako, Saitama 351-0198, Japan
[e] Department of Nephrology, Fujita Health University School of Medicine, Toyoake, Aichi 470-1192, Japan

ARTICLE INFO

Article history:
Received 19 October 2017
Accepted 30 October 2017
Available online xxx

Keywords:
Nucleotide sugar
UDP-mannose
Mannosylation
LC-ESI-MS/MS
Hypothalamus
Neocortex

ABSTRACT

Mannosylation in the endoplasmic reticulum is a key process for synthesizing various glycans. Guanosine diphosphate mannose (GDP-Man) and dolichol phosphate-mannose serve as donor substrates for mannosylation in mammals and are used in *N*-glycosylation, *O*-mannosylation, *C*-mannosylation, and the synthesis of glycosylphosphatidylinositol-anchor (GPI-anchor). Here, we report for the first time that low-abundant uridine diphosphate-mannose (UDP-Man), which can serve as potential donor substrate, exists in mammals. Liquid chromatography-mass spectrometry (LC-MS) analyses showed that mouse brain, especially hypothalamus and neocortex, contains higher concentrations of UDP-Man compared to other organs. In cultured human cell lines, addition of mannose in media increased UDP-Man concentrations in a dose-dependent manner. These findings indicate that in mammals the minor nucleotide sugar UDP-Man regulates glycosylation, especially mannosylation in specific organs or conditions.

1. Introduction

Glycosylation of proteins and lipids is vitally important in many biological processes. Dysregulation of glycosylation is associated with various diseases, such as diabetes mellitus, cancer, and degenerative neuromuscular disease [1–4]. Mannosylation occurring in the endoplasmic reticulum (ER) plays a key role in the synthesis of multiple types of glycans. Dolichol-linked mannose (Dol-P-Man) and GDP-mannose (GDP-Man) are donor substrates for mannosylation. Dol-P-Man is synthesized from mannose-6-phosphate via several intermediates (e.g., GDP-Man) of mannose metabolism [5]. These intermediates are also used in *N*-glycosylation, synthesis of GPI-anchor, *O*-mannosylation, and *C*-mannosylation.

With *N*-glycosylation Dol-P-Man and GDP-Man concentrations regulate mannosylation in the highly organized biosynthesis of *N*-glycan precursors, dolichol-linked oligosaccharides (DLOs). DLO biosynthesis is sensitive to the cellular metabolic states of monosaccharides. For example, glucose deprivation reduces GDP-Man concentrations, which in turn leads to the biosynthetic arrest of DLOs [6,7]. This facilitates the premature degradation of DLOs by pyrophosphatase [8]. This serves as a quality control system that prevents abnormal *N*-glycosylation [8].

Dol-P-Man deficiencies related to genetic factors cause congenital disorders of glycosylation (CDG), resulting in severe clinical symptoms [9]. For example, PMI-CDG and PMM2-CDG subtypes are caused by genetic mutations in phosphomannose isomerase and phosphomannomutase 2. Both of these enzymes are

* Corresponding author.
E-mail addresses: dglycotani@riken.jp, rvw.tani@sanken.osaka-u.ac.jp (N. Taniguchi).

https://doi.org/10.1016/j.bbrc.2017.10.173
0006-291X/

The abbreviations used

CDG	congenital disorders of glycosylation
CMP-NeuAc	cytidine monophospho N-acetyl-D-neuraminic acid
Dol-P-Man	dolichol-phosphate-mannose
DLO	dolichol-linked oligosaccharide
ESI-MS/MS	electrospray ionization-tandem mass spectrometry
GDP-Man	guanosine diphosphate mannose
GDP-Fuc	guanosine diphosphate fucose
GPI-anchor	glycosylphosphatidylinositol-anchor
LC-MS	liquid chromatography-mass spectrometry
MEF	mouse embryonic fibroblast
NMR	nuclear magnetic resonance
UDP-Gal	uridine diphosphate galactose
UDP-Glc	uridine diphosphate glucose
UDP-GlcA	uridine diphosphate glucuronic acid
UDP-HexNAc	uridine diphosphate N-acetyl hexosamine
UDP-Man	uridine diphosphate mannose
UDP	uridine diphosphate
UMP	uridine monophosphate

involved in GDP-Man biosynthesis [10,11]. In PMI-CDG patients, oral mannose supplementation restores normal glycosylation. Symptoms are relieved, because mannose can be converted to GDP-Man [10]. In mouse models of autoimmune diabetes and airway inflammation, oral mannose supplementation induces regulatory T cells and suppresses the immunopathology [12]. Genetic mutations associated with Dol-P-Man biosynthesis give rise to a high incidence of α-dystroglycanopathy [13–15]. This is caused by a deficiency of O-mannosyl glycans on α-dystroglycan in brain, peripheral nerves, and skeletal muscle [16,17]. Indeed, mannosylation is vital for mammalian development and cellular homeostasis. However, the precise roles of nucleotide sugar metabolism in regulating mannosylation are still not fully understood, particularly in *O*-mannosylation, GPI-anchor synthesis, and *C*-mannosylation.

In mammals, at least 12 types of nucleotide sugars are known. In contrast many more nucleotide sugars have been identified in plants and bacteria. At least 30 types of low-abundant nucleotide sugars exist in plants, and 70 nucleotide sugars have been identified in bacteria [18–21]. This disparity between mammals and plants and bacteria raises the possibility that minor nucleotide sugars remain to be identified in mammals. Indeed, low-abundant nucleotide sugars like UDP oligosaccharides are found in human milk [22,23].

We previously developed two methods for monitoring nucleotide sugar metabolism by using ion-pair reversed-phase LC and LC-electrospray ionization-tandem mass spectrometry (ESI-MS/MS) [24,25]. With these methods, cellular concentrations of abundant nucleotide sugars in mammalian cell lines were determined simultaneously [24]. In the present study, we sought to identify and measure low-abundant nucleotide sugars using these methods. We detected a nucleotide sugar that increases in concentration in mannose-rich media and found this nucleotide to be UDP-Man. We also determined UDP-Man concentrations in several human cell lines and mouse tissues, which led to the revelation that UDP-Man likely plays a unique role in glycosylation in specific mammalian organs, including brain.

2. Materials and methods

2.1. Materials

Uridine-5-diphospho-α-D-mannopyranoside (UDP-Man) was purchased from Sigma Aldrich Japan (Tokyo, Japan). Ammonium bicarbonate, acetonitrile, and distilled water were of LC-MS grade (Thermo Fisher Scientific, Waltham, MA). Triethylamine and formic acid of LC-MS grade were purchased from Wako Chemicals (Osaka, Japan). The sources of other materials were as follows: high-glucose DMEM (Sigma Aldrich, Japan); fetal bovine serum (Biowest, Nuaillé, France); glucose-free DMEM, penicillin, and streptomycin sodium salt (Life Technologies, Carlsbad, CA); all other chemicals (Wako Chemicals, Osaka, Japan).

2.2. Cell lines and animals

The human hepatoma cell line Hep3B, human breast cancer cell line MCF7, and the human lung adenocarcinoma epithelial cell line A549 were obtained from the ATCC (Manassas, VA). Human pancreatic cancer cell line PK8 was obtained from the Cell Resource Center for Biomedical Research Institute of Development, Aging, and Cancer (Tohoku University, Miyagi, Japan). Mouse embryonic fibroblast (MEF) cells were cultured and maintained as described previously [26]. Inadvertent mycoplasma infection of the MEF cell line was detected using e-MycoTM plus Mycoplasma PCR detection kit (iNtRON Biotechnology Inc, Jungwong-gu, Seongnam, Korea). Genomic DNA in harvested MEF cells was extracted using the i-genomic CTB DNA Extraction Mini Kit (iNtRON Biotechnology Inc., Korea).

Cell lines were cultured in high-glucose DMEM supplemented with 10% fetal bovine serum, 100 U/mL penicillin, and 100 μg/mL streptomycin until they reached approximately 60–70% confluence. To produce nucleotide sugars in the cell cultures, the culture medium was replaced with low glucose DMEM supplemented with mannose at various concentrations, ranging up to 20 mM. Then, the cells were maintained in culture for 3, 6, 12, or 24 h, followed by cell extraction and analysis (below).

All animal experiments were performed in compliance with the Institutional Guidelines for Animal Experiments of RIKEN. RIKEN institutional policies are consistent with ARRIVE Guidelines and follow international standards. To assess the regional distribution of UDP-Man in different organs, we used four 10-week-old male C57BL/6N mice (Charles River, MA). Mice were deeply anesthetized, and the liver, lung, brain, and kidney were extirpated immediately, and then placed into liquid nitrogen. The brain was further divided into seven parts according to standard anatomical regions: olfactory bulb, hypothalamus, cerebellum, medulla oblongata, hippocampus, neocortex, and “other” brain regions not included in the first six.

2.3. Preparation of cellular extracts from cultured cells and mouse tissues

Nucleotide sugars were prepared from the cultured cells (6-cm diameter dish), according to a previous report [24]. Cells were collected in ice-cold 70% ethanol (2 ml); and GDP-Glc (500 pmol) was added as an internal standard. The extract was centrifuged at 16,000 g for 15 min at 4 °C, and the supernatant was lyophilized. The freeze-dried samples were subjected to solid-phase extraction using an Envi-Carb column (100 mg; Supelco Inc, Bellafonte, PA). For mouse tissue samples, blocks of same-organ samples (30–90 mg) were manually homogenized in ice-cold 75% ethanol, and the tissue homogenates were prepared similarly to that described for cells. An Envi-Carb column (250 mg) was used also for

Please cite this article in press as: K. Nakajima, et al., Identification and characterization of UDP-mannose in human cell lines and mouse organs: Differential distribution across brain regions and organs, Biochemical and Biophysical Research Communications (2017), https://doi.org/10.1016/j.bbrc.2017.10.173

tissue samples.

2.4. Ion-pair reversed-phase LC-ESI-MS/MS

Ion-pair reversed-phase LC-ESI-MS/MS was performed using an Agilent 1100 series HPLC system (Agilent Technologies, Santa Clara, CA) coupled to an Esquire HCT ion trap mass spectrometer (Bruker Daltonics, Germany), according to a previously published method [25,27]. Cellular extracts were separated on an Inertsil ODS-3 column (3 μm, 150 × 2.1 mm, GL Science, Fukushima, Japan). Elution buffers were: (A) 20 mM triethylammonium acetate (TEAA) buffer, pH 6.0; and (B) buffer A containing 20% acetonitrile [25]. Portions of cellular extracts were analyzed by MS/MS analysis. For quantification, we calculated the peak area of extracted ion chromatograms of the major product ions. MS/MS transition for CMP-NeuAc was defined as *m/z* 613 to *m/z* 322, corresponding to a $[CMP]^-$ ion. Other nucleotide sugars were as follows: *m/z* 565/*m/z* 323 for UDP-Gal and UDP-Glc; *m/z* 606/*m/z* 385 for UDP-HexNAc; *m/z* 604/*m/z* 442 for GDP-Man; *m/z* 604/*m/z* 362 for GDP-Glc; *m/z* 579/*m/z* 323 for UDP-GlcA; and *m/z* 588/*m/z* 442 for GDP-Fuc. UDP-Man was monitored based on the characteristic fragment ion of *m/z* 565/*m/z* 403. Nucleotide sugar concentrations were normalized from the recovery of exogenous GDP-Glc and then expressed as pmol/mg protein.

2.5. Isolation of UDP-Man in mammalian cell lines

We prepared a mixture of nucleotide sugars from MEFs. For starting material, we cultured large amounts (5 × 15-cm diameter dishes) of MEFs in low glucose DMEM supplemented with 20 mM mannose. Extracts from the cells were then subjected to preparative HPLC under slightly modified conditions as those in Ref. [27]. After cell extraction, the extracts were fractionated by ion-pair reversed-phase LC by monitoring the ultraviolet absorption at 254 nm. To separate UDP-Man from CMP-NeuAc, we used the following: (A) elution buffer (20 mM TEAA buffer, pH 5.2); and (B) buffer A containing 20% acetonitrile. The fractionated solutions were lyophilized and analyzed by ion-pair reversed-phase LC, as reported previously [24].

Isolated UDP-Man (500 pmol) was hydrolyzed under acidic conditions with 0.02 M HCl (20 μL) at 100 °C for 20 min, and the pH of the samples was neutralized with 0.02 M NaOH [22]. A portion of the hydrolysate was analyzed by ion-pair reversed-phase LC [24].

2.6. NMR

NMR spectra were recorded with a 600-MHz NMR spectrometer (BrukerBioSpin, Osaka, Japan) equipped with a 5-mm TXI probe (Bruker). The probe temperature was set at 25 °C. The sample (200–500 nmol) was dissolved in 600 μL of D_2O (99.99 atom %D). One-dimensional ^{1}H-NMR spectra were collected with presaturation of the HDO signal. ^{1}H chemical shifts were reported relative to the external standard 4,4-dimethyl-4-silapentane-1-sulfonic acid. The NMR data were processed with TopSpin (version 2.1; Bruker), and the spectra were displayed using XWIN-PLOT (version 3.5; Bruker).

3. Results

3.1. LC-MS detection of UDP-Man induced in cells cultured in mannose-rich media

We first searched for the existence of low-abundant nucleotide sugars using ion-pair reversed-phase ESI-MS/MS using procedures in previous reports [24,25,27]. This system provides good sensitivity of nucleotide sugars at a level of 10 femtomoles and better separation based on the sugar motif (UDP-Gal and UDP-Glc). Furthermore, the MS/MS analysis of the deprotonated ion $[M-H]^-$ of UDP-hexose in the negative ion mode identifies molecules based on their characteristic fragment ions. This is because the fragment pattern in UDP-hexose is dependent on the *cis*/*trans* anomeric configuration of the phosphate group and 2-hydroxyl group of the hexose motif [28]. Because UDP-Glc and UDP-Gal produce one major fragment ion of $[UMP]^-$ at *m/z* 323, we were able to trace UDP-Glc and UDP-Gal with the *cis*-configuration by monitoring mass chromatograms of *m/z* 565/*m/z* 323 (Fig. S1). In contrast, UDP-Man (commercially available standard) with the *trans*-configuration was detected by the characteristic fragment ion of $[UDP]^-$ at *m/z* 403 (Fig. S1).

We analyzed cellular extracts from a hepatoma cell line (Hep3B) and MEFs after mannose supplementation, because these cells likely incorporate mannose efficiently via mannose-specific transporters [29]. Other cancer cell lines were also analyzed to test whether UDP-Man is distributed ubiquitously in other species and tissues (Fig. S2). Interestingly, in the Hep3B cell line cultured in the presence of 20 mM mannose, an unexpected additional peak was reliably detected at *m/z* 565/*m/z* 403 after ~8 min. This peak was barely detectable in mannose-free media (Fig. 1), implying that this peak reflects UDP-Man. The unexpected additional peak at *m/z* 565/*m/z* 323 was weakly detected because of the presence of abundant UDP-Gal and UDP-Glc, even though the molecule was increased in mannose-rich media.

3.2. Isolation and characterization of UDP-Man

The additional prominent peak detected at *m/z* 565/*m/z* 403 was very clear in several cell lines cultured in mannose-rich conditions (Fig. S2). Thus, we characterized the structure of the molecule by purifying the nucleotide sugars from extracts of MEFs. The purified nucleotide sugar showed a single peak in the HPLC chromatogram

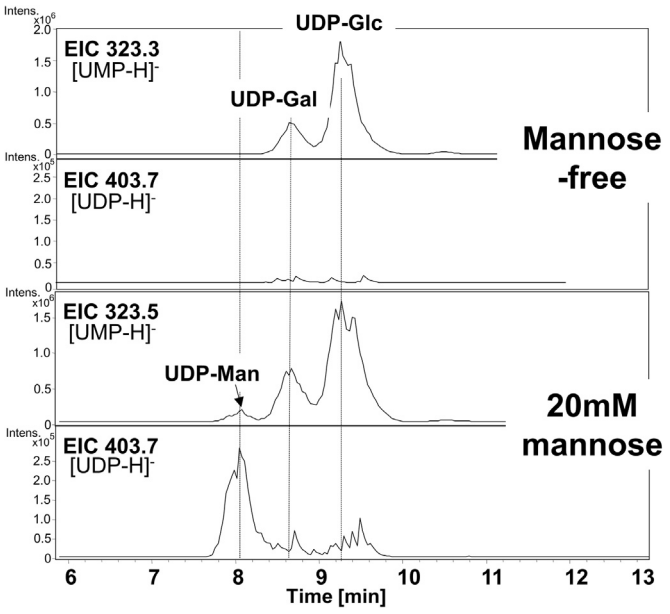

Fig. 1. Detection of UDP-Man in a mammalian hepatoma cell line cultured in mannose-rich media. Mass chromatograms of UDP-Man, UDP-Glc, and UDP-Gal. The concentrations of these compounds were measured at *m/z* 565/*m/z* 403 for UDP-Man, and at *m/z* 565/*m/z* 323 for UDP-Glc and UDP-Gal. Hep3B cells were cultured in low-glucose media supplemented with 20 mM mannose media or in low-glucose media lacking mannose for 24 h.

Please cite this article in press as: K. Nakajima, et al., Identification and characterization of UDP-mannose in human cell lines and mouse organs: Differential distribution across brain regions and organs, Biochemical and Biophysical Research Communications (2017), https://doi.org/10.1016/j.bbrc.2017.10.173

(Fig. 2A, bottom line), corresponding to the reference standard of UDP-Man (Fig. 2A, top line). We then subjected the fraction to ^{1}H-NMR analysis. The spectral pattern and chemical shift of the sample are almost identical to those of standard UDP-α-D-mannose (Fig. 2B, and Table S1), suggesting that the fraction contains UDP-α-D-mannose.

To further investigate the nucleotide motif, the purified nucleotide sugar was hydrolyzed under acidic conditions. Elution times of the major hydrolysates corresponded to UMP and UDP (Fig. 2A, middle line). These results clearly demonstrate that the additional peak found in mannose-treated cells was UDP-Man.

3.3. Nucleotide sugar concentrations in cells cultured in mannose-free or mannose-rich media

To test whether there is a dose-dependent relationship between increases in UDP-Man and mannose concentrations, we quantified nucleotide sugar concentrations in cells cultured in mannose-rich media (Table 1). The other nucleotide sugars, CMP-NeuAc, UDP-HexNAc, GDP-Man, UDP-GlcA, and GDP-Fuc, were assigned and quantified based on available reference standards as well as on MS/MS analysis (Fig. S3). With 20 mM mannose, the concentration of UDP-Man increased in all cell lines, although this increase differed among cell lines (Fig. S2). UDP-Man concentrations were remarkably elevated within 3 h of culturing the cells with mannose

Table 1
Nucleotide sugar concentrations in Hep3B cultured in mannose-free or mannose-rich media.

	Nucleotide sugar concentrations (pmol/mg protein)	
	Mannose-free media	20 mM Mannose-rich media
CMP-NeuAc	137 ± 24	111 ± 40
UDP-Man	0.76 ± 0.28	515 ± 26
UDP-Gal	739 ± 9	1417 ± 72
UDP-Glc	2449 ± 100	4132 ± 551
UDP-HexNAc	2110 ± 44	1119 ± 132
GDP-Man	16.2 ± 7.1	33.7 ± 1.0
UDP-GlcA	423 ± 43	695 ± 143
GDP-Fuc	263 ± 5	363 ± 23

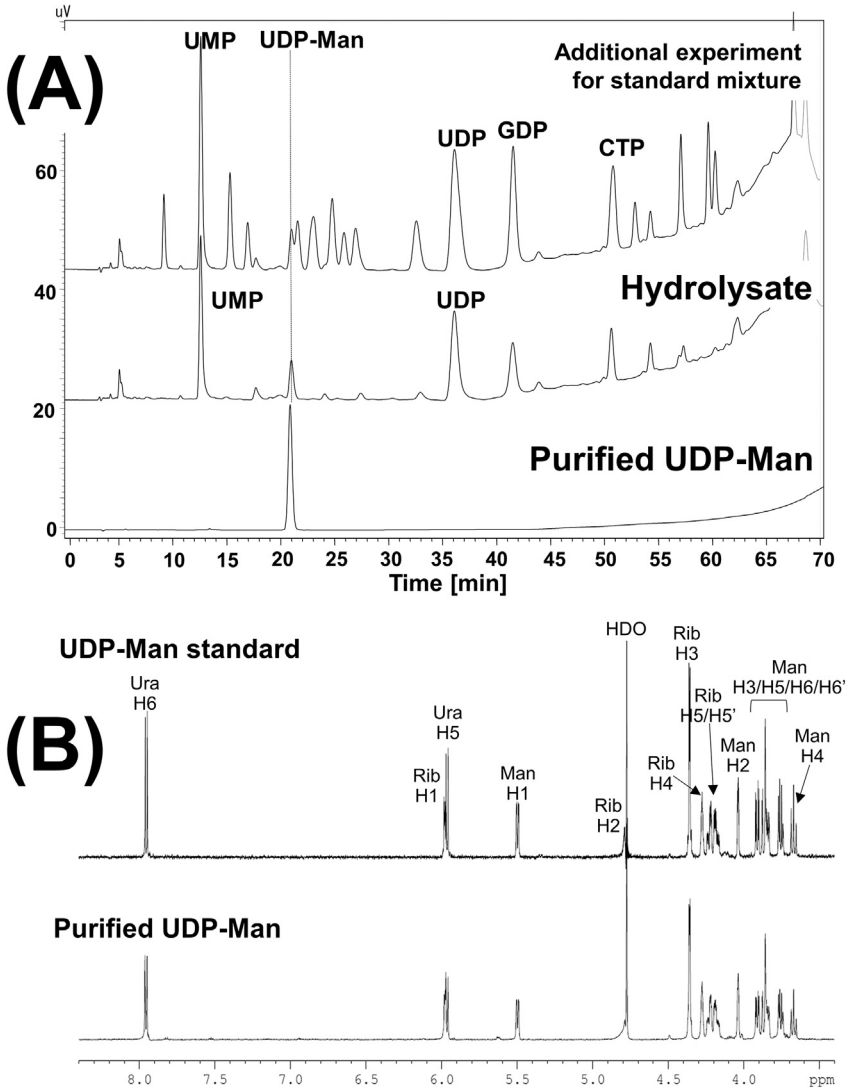

Fig. 2. Identification of purified UDP-Man. (A) Ion-pair reversed-phase LC profiles of purified UDP-Man and hydrolysates produced through acid hydrolysis. The upper profile represents the result of additional experiments involving mixtures of 20 different types of nucleotide sugars and nucleotides. Arrows indicate the elution positions of authentic compounds (UDP-Man, UMP, and UDP). (B) The 600 MHz ^{1}H-NMR spectra of UDP-Man (standard, 200–400 nmol) and purified UDP-Man (500 nmol) dissolved in D_2O. Probe temperature was set at 298 K. The residual HDO signal was suppressed using presaturation.

Please cite this article in press as: K. Nakajima, et al., Identification and characterization of UDP-mannose in human cell lines and mouse organs: Differential distribution across brain regions and organs, Biochemical and Biophysical Research Communications (2017), https://doi.org/10.1016/j.bbrc.2017.10.173

concentrations ranging from 0.2 to 20 mM (Fig. S4). With mannose-free media, the fragment ion at *m/z* 403, representing UDP-Man, was barely detectable (Fig. S5). For Hep3B cells cultured with 20 mM mannose, UDP-Man concentration increased by 650-fold compared to that in mannose-free media (Table 1). GDP-Man concentration increased only slightly in a mannose dose-dependent manner. For Hep3B cells cultured in mannose-free media, the UDP-Man concentration was 20- to 50-fold lower than GDP-Man concentration. Other nucleotide sugars showed moderate changes. UDP-GlcNAc concentration, for example, decreased by 50% when the cells were cultured in the presence of 20 mM mannose, while UDP-Glc, UDP-Gal, and UDP-GlcA concentrations increased (Table 1). The overall changes in nucleotide sugar concentrations are consistent with those reported previously [30].

3.4. Distribution in different organs

We next quantified UDP-Man concentrations in mouse liver, brain, lung, and kidney. For each tissue sample, three separate preparations were analyzed. The concentration of UDP-Man was markedly different in different organs (Fig. 3A). Brain, for example, had ~10-fold higher concentration of UDP-Man compared to other organs. The GDP-Man concentration in brain was 3-fold higher compared to that in other organs. GDP-Fuc and UDP-HexNAc concentrations were slightly higher than that of UDP-Man across the tissues analyzed, and quite similar to those reported previously [31]. The UDP-GlcNAc:UDP-GalNAc ratio is known to be constant (2.3–2.7) across different tissues [24]. However, we found that UDP-Man:GDP-Man ratios in the liver, brain, lung, and kidney varied, showing ratios of 1:71.3, 1:20.4, 1:30.4, and 1:9.0, respectively.

We further tested whether UDP-Man distribution differed depending on brain region. UDP-Man concentration was quantified in olfactory bulb, hypothalamus, cerebellum, medulla oblongata, hippocampus, neocortex, and other regions (i.e., other combined brain regions not in the six listed) of adult mice. UDP-Man concentrations was distinctly different across regions. Hypothalamus and neocortex were especially rich in UDP-Man, but olfactory bulb and cerebellum were poor. In contrast, GDP-Man concentration was similar across regions. The UDP-Man:GDP-Man ratios were highest in hypothalamus (1:7), implying that high ratios of UDP-Man to GDP-Man may reflect a potential donor substrate function for mannosyltransferases in hypothalamus.

4. Discussion

We have demonstrated for the first time the presence of a minor nucleotide sugar, UDP-Man, in mammals. Ion-pair reversed-phase LC-ESI-MS/MS identified UDP-Man in mouse brain, liver, and kidney. NMR analysis identified the structure of purified UDP-Man from a cell line cultured in mannose-rich media. The MS/MS analysis of the deprotonated ion $[M-H]^-$ at *m/z* 565 and the monitoring of the characteristic fragment ions of $[UDP]^-$ at *m/z* 403 facilitated the detection of the UDP-Man peak in mammalian sources (Fig. 1). The ion-pair reversed-phase mode also enabled the separation of UDP-Man from other nucleotide sugars, which facilitated the identification and purification of UDP-Man.

UDP-Man was detected in Hep3B, MCF7, A549, and PK8 cell lines in very small amounts, and its concentrations were elevated in cells grown in mannose-rich media (Table 1). While our study is the first to identify UDP-Man in mammals, “UDP-Man” has been reported in a few microbes. Singh and Hogan reported that UDP-Man in

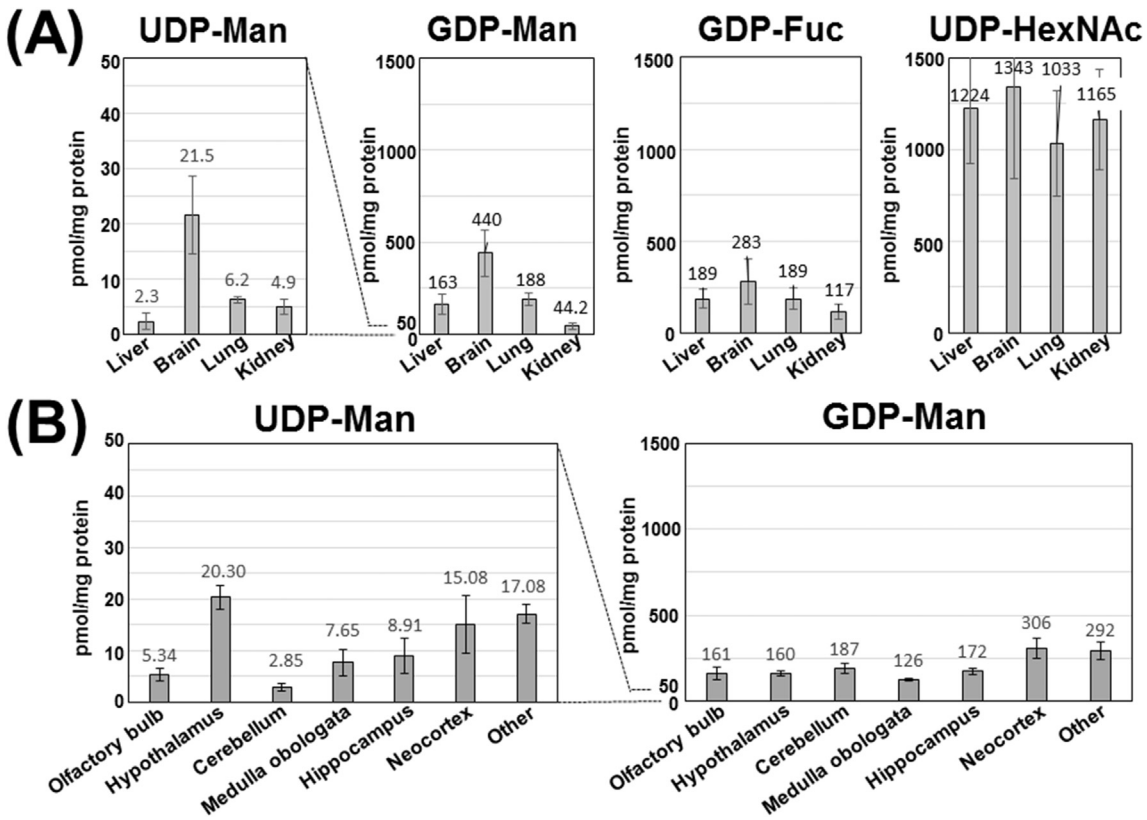

Fig. 3. UDP-Man, GDP-Man, GDP-Fuc, and UDP-HexNAc concentrations in different mouse organs. (A) Liver, brain, lung, and kidney. (B) Different regions of mouse brain. Independent samples were analyzed ($n = 4$), and the data were normalized to units of pmol/mg protein.

Please cite this article in press as: K. Nakajima, et al., Identification and characterization of UDP-mannose in human cell lines and mouse organs: Differential distribution across brain regions and organs, Biochemical and Biophysical Research Communications (2017), https://doi.org/10.1016/j.bbrc.2017.10.173

Mycobacterium smegmatis may be involved in the synthesis of mycobacterial polysaccharides [32]. We do not believe the UDP-Man we identified in our cell cultures spuriously derives from inadvertent bacterial contamination for several reasons. First, the tissue samples were taken from mice under SPF sterile conditions and immediately frozen before use. Second, cell lines were cultured in the presence of antibiotics. Third, we proactively tested for mycoplasma infection, and none could be detected in the MEF cell line (Fig. S6). Although there remains a slight possibility that the UDP-Man we identified derived from undetected bacterial contamination, the possibility is negligible.

In mammals, the metabolism of major nucleotide sugars metabolism has been established [18,20,21]. However, relatively small numbers of nucleotide sugars are involved in glycosylation in mammals compared to that in other organisms. Therefore, this newly detected UDP-Man could also serve as a potential donor substrate for mannosyltransferases and, as such, be a novel regulator of mannosylation.

We found that UDP-Man and GDP-Man concentrations vary across several different mouse organs, whereas UDP-HexNAc concentrations do not (Fig. 3). GDP-Man:UDP-Man ratios were quite different across the regions examined, implying that each nucleotide sugar may be synthesized via different pathways. Since identified UDP-α-D-Man is linked via α-linkage, like UDP-Glc and UDP-Gal, UDP-Man might be synthesized in a similar alternate pathway via UDP-glucose pyrophosphorylase or UDP-galactose pyrophosphorylase. Determining the key enzymes involved in UDP-Man synthesis is an important future step.

How does glycosylation via UDP-Man occur? Adamany et al. assessed the donor specificities of a thyroid mannosyltransferase in an *in vitro* enzymatic reaction and found that the relative activity toward UDP-Man is 45% of that toward GDP-Man in glycoprotein synthesis [33]. Although the UDP-Man concentration was quite low when compared to GDP-Man concentration (Fig. 3 and Table 1), UDP-Man is possibly involved not only in *N*-glycosylation but also in other glycosylations (e.g., synthesis of GPI-anchor, and *O*- and *C*-mannosylation).

Is glycosylation via UDP-Man more important in particular tissues? Interestingly, we observed characteristic differential distribution of UDP-Man. UDP-Man concentrations are greater in the hypothalamus and neocortex compared to other brain regions (Fig. 3). Thus, this pattern may reflect functional differences in glycosylation occurring through UDP-Man in the brain. For example, hypothalamus-specific function might be relevant to metabolic regulation due to active glucose metabolism in the brain. Thus, investigating the biological significance and functions of UDP-Man in mammals may pose many challenges because of its low abundance. However, given its roles in quality control of glycosylation [8], and immune system function [12], a better understanding of glycosylation via UDP-Man in humans may open up new avenues for treating neurological disease.

In conclusion, the detection of UDP-Man in mammalian tissues provides new insights into understanding the regulatory mechanisms of glycosylation.

Conflict of interest

The authors declare no conflicts of interest.

Acknowledgments

We thank Dr. Takashi Angata (Academia Sinica, Taiwan) and Dr. Kazuaki Ohtsubo (Kumamoto University) for helpful suggestions on research designs, and Dr. Masanori Kugita (Fujita Health University) and Ms. Mizuki Kurosawa (RIKEN, BSI) for technical support with the animal experiments. This work was supported by Grant-in-Aid for Young Scientists (B), 24790301 (to KN) and Grant-in-Aid for Scientific Research (B), 15H04700 (to NT) from the Ministry of Education, Culture, Sports, Science and Technology of Japan.

Appendix A. Supplementary data

Supplementary data related to this article can be found at https://doi.org/10.1016/j.bbrc.2017.10.173.

References

[1] K. Ohtsubo, J.D. Marth, Glycosylation in cellular mechanisms of health and disease, Cell 126 (2006) 855–867.
[2] S. Hakomori, Aberrant glycosylation in tumors and tumor-associated carbohydrate antigens, Adv. Cancer Res. 52 (1989) 257–331.
[3] N. Taniguchi, Y. Kizuka, Glycans and cancer: role of N-glycans in cancer biomarker, progression and metastasis, and therapeutics, Adv. Cancer Res. 126 (2015) 11–51.
[4] R. Kleene, M. Schachner, Glycans and neural cell interactions, Nat. Rev. Neurosci. 5 (2004) 195–208.
[5] V. Sharma, M. Ichikawa, H.H. Freeze, Mannose metabolism I: more than meets the eye, Biochem. Biophys. Res. Commun. 453 (2014) 220–228.
[6] J.I. Rearick, A. Chapman, S. Kornfeld, Glucose starvation alters lipid-linked oligosaccharide biosynthesis in Chinese hamster ovary cells, J. Biol. Chem. 256 (1981) 6255–6261.
[7] H. Gershman, P.W. Robbins, Transitory effects of glucose starvation on the synthesis of dolichol-linked oligosaccharides in mammalian cells, J. Biol. Chem. 256 (1981) 7774–7780.
[8] Y. Harada, K. Nakajima, Y. Masahara-Negishi, H.H. Freeze, T. Angata, N. Taniguchi, T. Suzuki, Metabolically programmed quality control system for dolichol-linked oligosaccharides, Proc. Natl. Acad. Sci. U.S.A. 110 (2013) 19366–19371.
[9] H.H. Freeze, Understanding human glycosylation disorders: biochemistry leads the charge, J. Biol. Chem. 288 (2013) 6936–6945.
[10] M. Niehues, et al., Carbohydrate-deficient glycoprotein syndrome type Ib. Phosphomannose isomerase deficiency and mannose therapy, J. Clin. Invest. 101 (1998) 1414–1420.
[11] E. Van Schaftingen, J. Jaeken, Phosphomannomutase deficiency is a cause of carbohydrate-deficient glycoprotein syndrome type I, FEBS Lett. 377 (1995) 318–320.
[12] D. Zhang, et al., D-mannose induces regulatory T cells and suppresses immunopathology, Nat. Med. 9 (2017) 1036–1045.
[13] A.C. Yang, et al., Congenital disorder of glycosylation due to DPM1 mutations presenting with dystroglycanopathy-type congenital muscular dystrophy, Mol. Genet. Metab. 110 (2013) 345–351.
[14] R. Barone, et al., DPM2-CDG: a muscular dystrophy-dystroglycanopathy syndrome with severe epilepsy, Ann. Neurol. 72 (2012) 550–558.
[15] D.J. Lefeber, et al., Deficiency of Dol-P-Man synthase subunit DPM3 bridges the congenital disorders of glycosylation with the dystroglycanopathies, Am. J. Hum. Genet. 85 (2009) 76–86.
[16] T. Endo, O-mannosyl glycans in mammals, Biochim. Biophys. Acta. 1473 (1999) 237–246.
[17] R. Barresi, K.P. Campbell, Dystroglycan: from biosynthesis to pathogenesis of human disease, J. Cell Sci. 119 (2006) 199–207.
[18] A. Varki, R.D. Cumming, J.D. Esko, H.H. Freeze, P. Stanley, C.R. Bertozzi, G.W. Hart, M.E. Etzler, Essentials of Glycobiology, second ed., Cold Spring Harbor, New York, 2008.
[19] M. Bar-Peled, M.A. O'Neill, Plant nucleotide sugar formation, interconversion, and salvage by sugar recycling, Annu. Rev. Plant Biol. 62 (2011) 127–155.
[20] E. Cabib, Carbohydrate metabolism, Ann. Rev. Biochem. 32 (1962) 321–354.
[21] R.H. Herman, Mannose metabolism, Am. J. Clin. Nutr. 24 (1971) 488–498.
[22] A. Kobata, Z. Suzuoki, M. Kida, The acid-soluble nucleotides of milk: I. Quantitative and qualitative differences of nucleotides constituents in human and cow's milk, J. Biochem. 51 (1962) 277–287.
[23] M. Sasaki, T. Nakamura, K. Hirayama, K. Fukuda, T. Saito, T. Urashima, S. Asakuma, Characterization of two novel sialyl N-acetyllactosaminyl nucleotides separated from ovine colostrum, Glycoconj. J. 5 (2016) 789–796.
[24] K. Nakajima, S. Kitazume, T. Angata, R. Fujinawa, K. Ohtsubo, E. Miyoshi, N. Taniguchi, Simultaneous determination of nucleotide sugars with ion-pair reversed-phase HPLC, Glycobiology 20 (2010) 865–871.
[25] K. Nakajima, E. Ito, K. Ohtsubo, K. Shirato, R. Takamiya, S. Kitazume, T. Angata, N. Taniguchi, Mass isotopomer analysis of metabolically labeled nucleotide sugars and N- and O-glycans for tracing nucleotide sugar metabolisms, Mol. Cell. Proteomics. 12 (2013) 2468–2480.
[26] X. Wang, et al., Dysregulation of TGF-beta1 receptor activation leads to abnormal lung development and emphysema-like phenotype in core fucose-deficient mice, Proc. Natl. Acad. Sci. U. S. A. 102 (2005) 15791–15796.
[27] D.C. Turnock, L. Izquierdo, M.A. Ferguson, The de novo synthesis of GDP-fucose is essential for flagellar adhesion and cell growth in *Trypanosoma brucei*, J. Biol. Chem. 282 (2007) 28853–28863.

Please cite this article in press as: K. Nakajima, et al., Identification and characterization of UDP-mannose in human cell lines and mouse organs: Differential distribution across brain regions and organs, Biochemical and Biophysical Research Communications (2017), https://doi.org/10.1016/j.bbrc.2017.10.173

[28] B.A. Wolucka, J.S. Rush, C.J. Waechter, V.N. Shibaev, E. de Hoffmann, An electrospray-ionization tandem mass spectrometry method for determination of the anomeric configuration of glycosyl-1-phosphate derivatives, Anal. Biochem. 255 (1998) 244–251.
[29] K. Panneerselvam, H.H. Freeze, Mannose enters mammalian cells using a specific transporter that is insensitive to glucose, J. Biol. Chem. 271 (1996) 9417–9421.
[30] T.A. Jokela, M. Jauhiainen, S. Auriola, M. Kauhanen, R. Tiihonen, M.I. Tammi, R.H. Tammi, Mannose inhibits hyaluronan synthesis by down-regulation of the cellular pool of UDP-N-acetylhexosamines, J. Biol. Chem. 283 (2008) 7666–7673.
[31] S. Oikari, T. Venäläinen, M.I. Tammi, Borate-aided anion exchange high-performance liquid chromatography of uridine diphosphate-sugars in brain, heart, adipose and liver tissues, J. Chromatogr. A 1323 (2014) 82–86.
[32] S. Singh, S.E. Hogan, Isolation and characterization of sugar nucleotides from Mycobacterium smegmatis, Microbios 77 (1994) 217–222.
[33] A.M. Adamany, R.G. Spiro, Glycoprotein biosynthesis: studies on thyroid mannosyltransferases. I. Action on glycopeptides and simple glycosides, J. Biol. Chem. 250 (1975) 2830–2841.

Please cite this article in press as: K. Nakajima, et al., Identification and characterization of UDP-mannose in human cell lines and mouse organs: Differential distribution across brain regions and organs, Biochemical and Biophysical Research Communications (2017), https://doi.org/10.1016/j.bbrc.2017.10.173